

## Article

# The Oxidation Performance of a Carbon Soot Catalyst Based on the Pt-Pd Synergy Effect

Diming Lou, Guofu Song, Kaiwen Xu, Yunhua Zhang \* and Kan Zhu

School of Automotive Studies, Tongji University, Shanghai 201800, China; loudiming@tongji.edu.cn (D.L.); 2180073@tongji.edu.cn (G.S.); xukaiwen@tongji.edu.cn (K.X.); zhuk\_74@tongji.edu.cn (K.Z.)

\* Correspondence: zhangyunhua@tongji.edu.cn

**Abstract:** Pt-Pd-based noble metal catalysts are widely used in engine exhaust aftertreatment because of their better carbon soot oxidation performance. At present, the synergistic effect of Pt and Pd in CDPFs, which is the most widely used and common doping method, in catalyzing the combustion of carbon smoke has not been reported, and it is not possible to give an optimal doping ratio of Pt and Pd. This paper investigates the carbon soot oxidation performance of different Pt/Pd ratios (Pt/Pd = 1:0, 10:1, 5:1, 1:1) based on physicochemical characterization and particle combustion kinetics calculations, aiming to reveal the Pt-Pd synergistic effect and its carbon soot oxidation law. The results show that Pt-based catalysts doped with Pd can improve the catalyst dispersion, significantly increase the specific surface area, and reduce the activation energy and reaction temperature of carbon soot reactions, but excessive doping of Pd leads to the enhancement of the catalyst agglomeration effect, a decrease in the specific surface area, and an increase in the activation energy and reaction temperature of the carbon soot reaction. The specific surface area and pore capacity of the catalyst are the largest, and the activation energy of particle oxidation and the pre-exponential factor are the smallest (203.44 kJ·mol<sup>-1</sup> and 6.31 × 10<sup>7</sup>, respectively), which are 19.29 kJ·mol<sup>-1</sup> and 4.95 × 10<sup>8</sup> lower than those of pure carbon soot; meanwhile, the starting and final combustion temperatures of carbon soot (T<sub>10</sub> and T<sub>90</sub>) are the lowest at 585.8 °C and 679.4 °C, respectively, which are 22.1 °C and 20.9 °C lower than those of pure carbon soot.



**Citation:** Lou, D.; Song, G.; Xu, K.; Zhang, Y.; Zhu, K. The Oxidation Performance of a Carbon Soot Catalyst Based on the Pt-Pd Synergy Effect. *Energies* **2024**, *17*, 1737. <https://doi.org/10.3390/en17071737>

Academic Editors: Kazimierz Lejda, Artur Jaworski and Maksymilian Mądziel

Received: 2 March 2024

Revised: 24 March 2024

Accepted: 26 March 2024

Published: 4 April 2024



**Copyright:** © 2024 by the authors. Licensee MDPI, Basel, Switzerland. This article is an open access article distributed under the terms and conditions of the Creative Commons Attribution (CC BY) license (<https://creativecommons.org/licenses/by/4.0/>).

**Keywords:** Pt-Pd synergy; carbon soot; physicochemical properties; combustion kinetics; oxidation properties

## 1. Introduction

Diesel engines with low fuel consumption, high torque, high reliability, and other advantages are widely used in road transport, marine transport, national defense equipment, non-road mobile machinery (construction machinery, agricultural machinery, generator sets, etc.), and other fields. All kinds of trucks and medium and large buses mainly use diesel engines as their power source. China has a vast territory and a large mountainous area, and both passenger and cargo transport mainly involve road transport. In 2021, road transport dominated by diesel vehicles bore about 61.2% of passenger transport and 73.8% of cargo transport [1], and for a long time, diesel power will still be the backbone of national defense equipment, economic development, and infrastructure construction. Compared with gasoline engines, the emission of pollutants has been one of the important factors that trouble the wide popularization of diesel engines. As a result of the growing number of motor vehicles and industrialization, air pollution has become an important environmental problem faced by all parts of the world. Diesel engines, as one of the important driving forces in modern society and an irreplaceable part of the human production process, are widely used in various domains such as transportation, industry, and agricultural production, and are also one of the main contributors to the air pollution problem. As emission regulations are constantly upgraded, emission requirements are also becoming stricter and stricter. Diesel National VI emission regulations are more stringent compared

to the National V emission limits and test methods. In diesel engine emissions, particulate matter (PM) emission is of concern. Diesel exhaust particles are mainly composed of non-volatile (insoluble) and volatile (soluble) parts. Volatile compounds are composed of organic carbon, sulfate, and nitrate compounds, while the non-volatile portion is composed of the carbonaceous (soot) portion and ash [2]. Particulate matter can be suspended in the air for a long time, polluting the environment and affecting human physical and mental health. The size of 70% of particles is less than  $0.3\ \mu\text{m}$ , mainly composed of carbon smoke particles and soluble organic fraction (SOF) with hydrocarbon droplets and sulfuric acid droplets adsorbed on the surface. These fine carbon smoke particles are easily inhaled by the human body in the alveoli and are difficult to eliminate. SOF and other chemicals adsorbed on the particles in particular will lead to toxic metals such as lead, cadmium, and zinc being absorbed into the blood through the respiratory tract and cause hypersensitivity and allergic reactions, which may also lead to bacterial and fungal infections in living organisms, as well as cancer, pulmonary fibrosis, and mucosal irritation [3]. At the same time, PM emitted by engine exhausts into the atmosphere becomes a pollutant and disturbs the atmospheric radiation balance, thus aggravating the effect of global warming [4].

For this reason, emission regulations strictly control particulate matter emissions from diesel vehicles. As a result, the Diesel Particulate Filter (DPF) is an essential device in diesel exhaust treatment systems, capturing particles through a mixture of surface and internal filters using methods such as such as diffusion precipitation, inertial precipitation, and linear interception. DPFs can effectively purify 65–90% of the particulates in exhaust gas, making it one of the most effective and direct methods to purify the particulates produced by diesel vehicles [5]. However, with the accumulation of DPF running time and mileage, a large number of particles will accumulate and block the DPF, which will increase the exhaust back pressure and lead to the deterioration of engine power performance and economic performance. Therefore, it is necessary to burn off the particles gathered on the surface of the DPF in a timely manner and carry out a regeneration treatment on the DPF. There are two regeneration methods for DPFs [6], namely active regeneration and passive regeneration. Because the combustion of particulate matter requires a very high temperature, much higher than the temperature of diesel engine exhausts, passive regeneration usually involves coating a catalyst on the surface of DPF carriers to reduce the combustion temperature of particulate matter so that it can be ignited and burned at a lower exhaust temperature.

The catalyst can participate in the process of the combustion reaction, reduce the activation energy of the chemical reaction, and accelerate the reaction rate. In the passive regeneration process of Catalyzed Diesel Particulate Filters (CDPFs), the catalyst plays a key role. The effect of passive regeneration often depends on the quality of the catalyst.

There are two types of catalysts currently used in CDPFs. The first type is a non-noble-metal catalyst without noble metal doping. Catalysts based on non-noble metals can be divided into the following main types: perovskite-type catalysts [7], spinel-type catalysts [8], and transition metal oxide catalysts. Among them, cerium dioxide-based catalysts [9,10] and other metal oxide catalysts [11–13] are represented. The other type of catalyst is the noble-metal-doped catalyst. The noble-metal catalyst is the most widely used CDPF catalyst, as it has the highest catalytic efficiency and best performance among catalysts. At present, the noble metals used mainly include Pt, Pd, Rh, and other elements. Usually, metal oxides such as alumina and titanium dioxide are used as the carriers of noble-metal catalysts. The carbon smoke particles on CDPFs can be effectively removed under the joint action of noble-metal elements and carriers. Moreover, relevant studies showed that [14] the activity of Pt supported on  $\text{TiO}_2\text{-SiO}_2$  (Pt/ $\text{TiO}_2\text{-SiO}_2$ ) was higher than those of other Pt/MOx systems (MOx =  $\text{TiO}_2$ ,  $\text{ZrO}_2$ ,  $\text{SiO}_2$ , MOX).  $\text{Al}_2\text{O}_3$ ,  $\text{TiO}_2\text{-ZrO}_2$ ,  $\text{TiO}_2\text{-Al}_2\text{O}_3$ ,  $\text{ZrO}_2\text{-SiO}_2$ ,  $\text{ZrO}_2\text{-Al}_2\text{O}_3$ , and  $\text{SiO}_2\text{-Al}_2\text{O}_3$  had higher activity. The form of carbon particle oxidation catalyzed by noble-metal catalysts is generally considered to be gas-phase catalysis [15]. Pt indirectly promotes the oxidation of soot; that is, it catalyzes the oxidation of NO in the exhaust gas to  $\text{NO}_2$  and then oxidizes the soot to  $\text{CO}_2$  [16,17].

Noble-metal (Ag, Pt, and Pd) catalysts using  $\text{CeO}_2$  and  $\text{TiO}_2$  as carriers showed higher particulate matter (PM) catalytic oxidation activity for Ag than for Pt and Pd under tight and loose contact conditions [18]. The thermal stability and catalytic activity of a Pt/ $\text{Al}_2\text{O}_3$  catalyst modified with Pd became better due to the addition of Pd [19]. A comparison of the isothermal oxidation kinetic properties (rate and activation energy) of soot with the physicochemical properties of diesel, charcoal, and commercial (Printex U, Vulkan XC-72, Mumbai, India) soot samples showed that the oxidative reactivity of soot depended on many parameters. The oxidative reactivity of soot on the surface of Pt-Pd/ $\text{MnOx-Al}_2\text{O}_3$  oxidation catalysts with low Pt-Pd content aimed at removing diesel soot depended on many parameters, but mainly on the nanostructure, microstructure, and composition of surface functional groups [20].

Worldwide, scholars have confirmed that DPF catalysts doped with Pt and other noble-metal elements have more obvious catalytic effects on soot combustion, and that such catalytic reactions are related to the microstructure of the catalysts, the functional groups on the surface of the catalysts, and the use of different elements in the doping. However, the synergistic effect of Pt and Pd in CDPFs catalyzing the combustion of soot, which is the most widely used and common doping method, has not yet been reported, and the optimal doping ratio of Pt and Pd could not be given.

Therefore, in this paper, four groups of DPF catalysts with different Pt and Pd content ratios are studied, the microscopic characteristics of the catalyst surface are characterized and analyzed, and the activation energy (E) and predigital factor (A) of the reaction catalyzed by soot are calculated using the Coats–Redfern integral method. At the same time, the influence of different Pt-Pd catalysts on the soot catalytic combustion of diesel engines is analyzed based on the key temperature of the soot combustion reaction.

## 2. Materials and Methods

Through scanning electron microscope (SEM) imaging and a specific surface area test (BET test), the micro photos and physical characteristics of the sample were obtained. Derivative thermogravimetric (DTG) curves, as well as the curves of mass and temperature (TG) and differential scanning calorimetry (DSC) were obtained by thermogravimetric testing and a differential scanning calorimetry test to describe the combustion kinetic characteristics of the sample.

### *Test Materials and Equipment*

According to the different content ratio of Pt and Pd in the catalyst, the test samples were divided into 4 types, as shown in Table 1. The soot used is 99% pure carbon powder. The mixed state of the catalyst and soot particles can be divided into tight contact and loose contact, which will have a great influence on the thermogravimetric results. The loose contact state was more consistent with the actual state on the DPF, and the loose contact mode was used in this study. The total mass of each test sample was 6 mg, the mass ratio of catalyst to carbon smoke was 1:1 (that is, the mass fraction of carbon smoke was 50%), and they were gently stirred evenly to ensure that the two were in loose contact (stirring for at least 3 min).

**Table 1.** Test samples.

Serial No.	Catalyst Proportioning
1	Pt/Pd = 1:0
2	Pt/Pd = 10:1
3	Pt/Pd = 5:1
4	Pt/Pd = 1:1

The instrument used for SEM analysis in this experiment was a Thermo Fisher Apreo2C scanning electron microscope (Waltham, MA, USA). The scanning electron microscope has a resolution of 1.2 nm at 1 kV, a landing energy range of 20 eV~30 keV, and a

maximum beam current of 50 nA. The BET data were determined using a NOVA-1200 spectrophotometer manufactured by Quantchrom (Boynton Beach, FL, USA). The instrument has a minimum measurable specific surface area value of  $0.01 \text{ m}^2/\text{g}$ , a measurable pore size range of 0.35 nm to  $>400 \text{ nm}$ , and a minimum pore volume of  $0.0001 \text{ cc/g}$ . Thermogravimetric testing was carried out with a TG209F1 Thermogravimetric Analyzer from NETZSCH (Selb, Bavaria, Germany). The thermogravimetric analyzer has a maximum sample mass of 2 g, a maximum temperature of  $1100 \text{ }^\circ\text{C}$ , an adjustable heating rate between  $0.001 \text{ K/min}$  and  $200 \text{ K/min}$ , and a TGA resolution of  $0.1 \text{ }\mu\text{g}$ . DSC tests were performed with a Synchronized Thermal Synthesis Analyzer (STA449F3) from NETZSCH (Selb, Bavaria, Germany). The analyzer has a temperature range of  $-150\sim 2400 \text{ }^\circ\text{C}$ , a temperature increase rate of up to  $50 \text{ K/min}$ , a maximum test sample mass of 35 g, and a test resolution of  $0.1 \text{ }\mu\text{g}$ .

In order to simulate the actual oxygen content of diesel exhaust gas, the set working atmosphere of the thermogravimetric test was 13%  $\text{O}_2$  and 87%  $\text{N}_2$  syngas. The working gas flow rate was  $50 \text{ mL/min}$ . The temperature rise rate was  $10 \text{ }^\circ\text{C/min}$ , and the temperature rise range was  $40\sim 800 \text{ }^\circ\text{C}$ . The TG curve, DTG curve, and DSC curve were obtained.

### 3. Results and Discussion

#### 3.1. Analysis of Catalyst Characterization Results

##### 3.1.1. Analysis of SEM Results

SEM images of the four catalysts are shown in Figure 1, and the surfaces of the catalysts of the four proportioning schemes showed good granularity. The catalyst surface had fine particles, fluffy organization, and a lot of pores, which increase the surface area of the catalyst, making the catalyst have a sufficient contact area with the carbon fume, and the catalytic effect of the catalyst is maximized.

The catalyst particles in the Pt/Pb = 1:0 scheme show a small state. When Pb is added, Pt/Pb = 10:1; the catalyst particles have a small increase, but at the same time, the particles are more loose from each other, and the pores are obviously increased. When Pb is further added, Pt/Pb = 5:1; the catalyst particles have an obvious effect of increasing, and the agglomeration effect occurs, which makes the surface area experience a small decrease. When Pt/Pb = 1:1, the catalyst particles further increase, resulting in a significant decrease in surface area.

When a small amount of the Pd element is added (Pt/Pb = 10:1), the particles on the surface of the catalyst are more dispersed, the granularity is more obvious, and the pores are more adequate, with a better synergistic effect. With the increase in the added Pd content, the particles on the catalyst surface have a tendency to re-colonize and become larger.

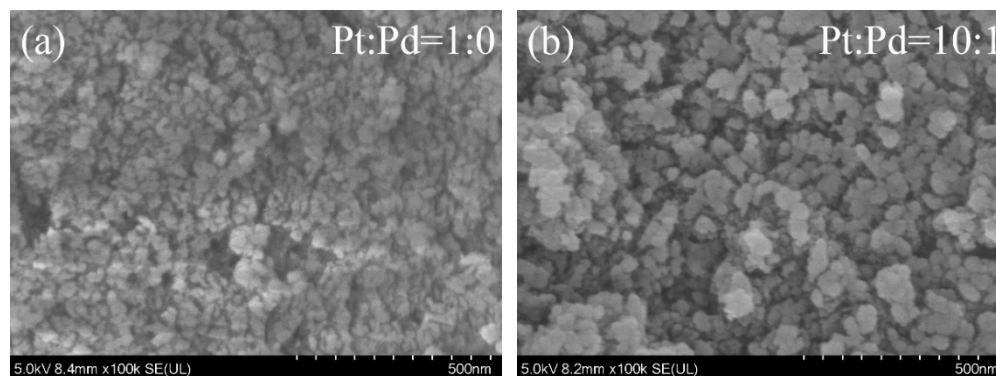
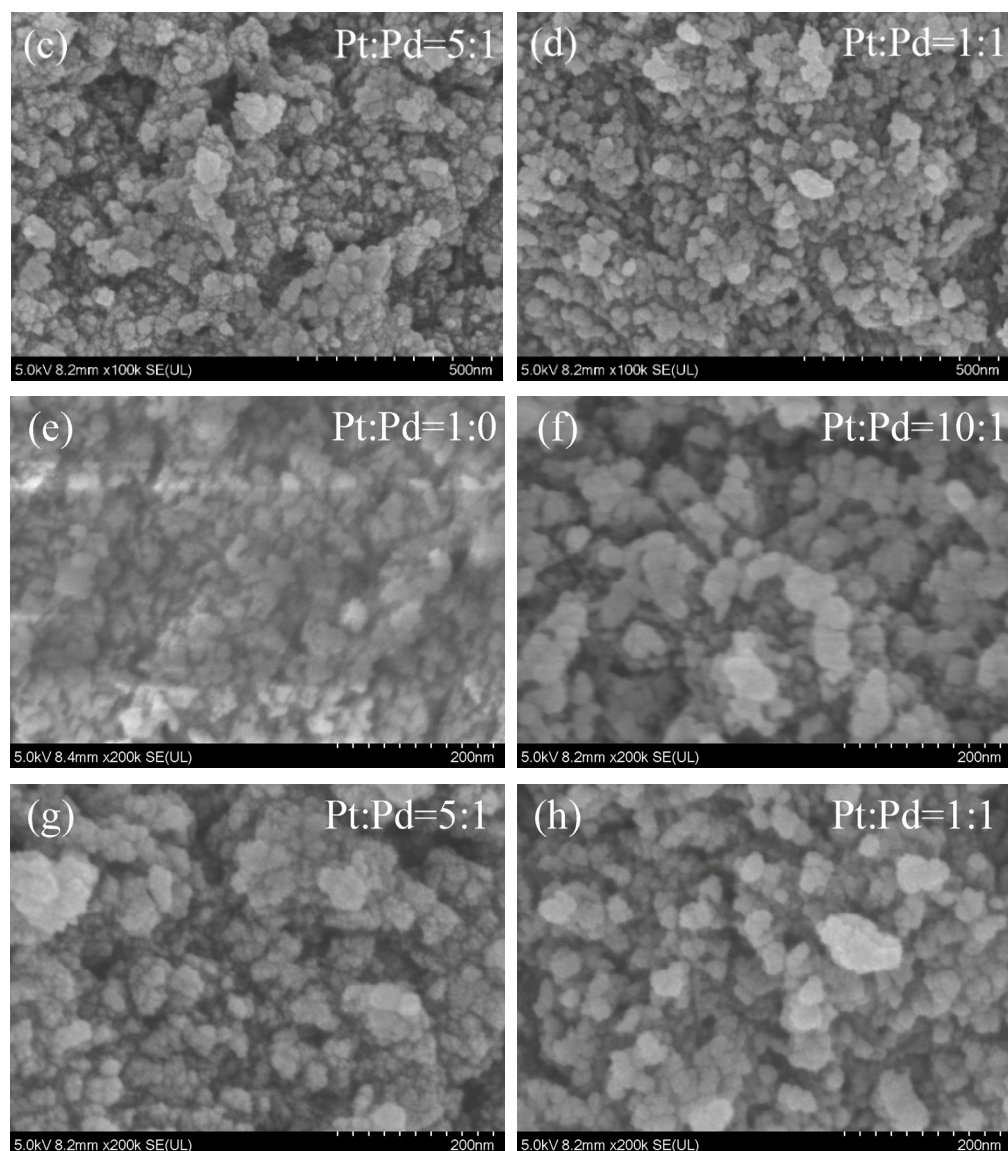


Figure 1. Cont.



**Figure 1.** SEM photos of the four catalysts.

### 3.1.2. Analysis of BET Results

The specific surface area and pore volume parameters of the four catalysts obtained after BET tests are shown in Table 2. The specific surface areas of the four catalyst schemes were more than  $110 \text{ m}^2/\text{g}$ , among which the Pt/Pd = 10:1 ratio scheme had the largest specific surface area of  $140.366 \text{ m}^2/\text{g}$ ; the Pt/Pd = 1:0 ratio scheme had the smallest specific surface area of  $113.842 \text{ m}^2/\text{g}$ . The pore volumes of the four catalyst schemes were the largest for the Pt/Pd = 10:1 ratio scheme at  $0.5359 \text{ cm}^3/\text{g}$ ; the Pt/Pd = 1:1 ratio scheme has the smallest pore volume of  $0.3644 \text{ cm}^3/\text{g}$ .

**Table 2.** BET results for the four proportioning schemes.

Catalyst	SBET ( $\text{m}^2/\text{g}$ )	Vp ( $\text{cm}^3/\text{g}$ )
Pt/Pd = 1:0	114	0.44
Pt/Pd = 10:1	140	0.54
Pt/Pd = 5:1	132	0.40
Pt/Pd = 1:1	116	0.36

According to the results in Table 2, a small amount of added Pd can increase the specific surface area and pore volume of the catalyst, but with the increase in Pd addition, both the specific surface area and pore volume decrease to different extents, and the pore volume decreases to lower than that of the un-added Pd solution after the ratio of Pt and Pd reaches or exceeds 5:1.

### 3.2. Analysis of Test Results

The TG curves, DTG curves, and DSC curves of the four catalyst ratios obtained from the experiments are shown in Figure 2, and the downward direction in the DSC curves is the exothermic direction. The maximum exothermic rates of each scheme are close to each other, among which the Pt/Pd = 5:1 scheme has the lowest maximum exothermic rate of 11.5 mW/mg and the Pt/Pd = 10:1 scheme had the highest maximum exothermic rate of 14.3 mW/mg.

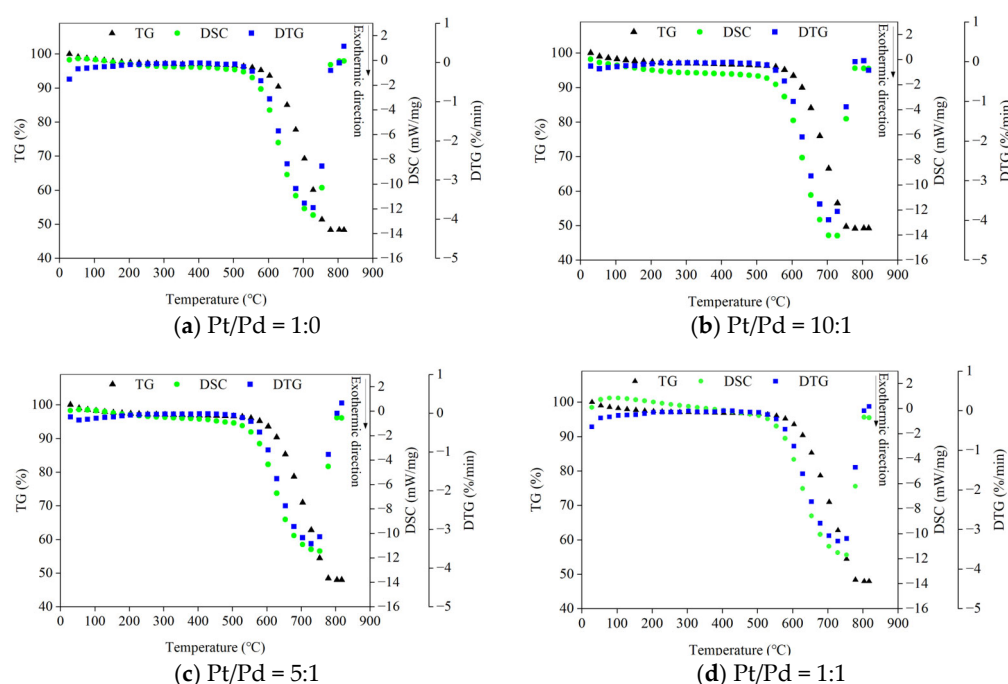


**Figure 2.** TG-DTG-DSC test curve.

### 3.3. Calculation of Kinetic Parameters and Combustion Temperature

#### 3.3.1. Analysis of SEM Results

In this paper, the thermodynamic parameters, such as the activation energy ( $E$ ) and pre-exponential factor ( $A$ ) of carbon black, were calculated using the Coats–Redfern integral method [21], and the effects of different Pt/Pd ratios on the catalytic oxidation characteristics and thermodynamic parameters of diesel particulate matter were analyzed based on the results.

The initial mass of the test sample is set to be  $m_0$ ; the sample is burned and consumed during the test, and the mass changes to  $m$  at time  $t$ . The final residual sample mass is  $m_e$ . Therefore, the combustion decomposition rate of the sample is

$$d\alpha/dt = kf(\alpha) \quad (1)$$

In Equation (1),  $\alpha$  is the sample conversion rate;  $\alpha = [(m_0 - m)/(m_0 - m_e)] \times 100\%$ ;  $t$  is the response time;  $k$  is the Arrhenius reaction rate constant;  $k = A \exp(-E/RT)$ ;  $A$  is the pre-exponential factor of an index;  $E$  is the activation energy;  $R = 8.314 \text{ J}/(\text{mol} \cdot \text{K})$  is the molar gas constant;  $T$  is the thermodynamic temperature; and  $f(\alpha)$  is the differential form of the reaction mechanism function. The reaction temperature is ramped up at a

certain rate of increase,  $\beta$ ; the expression is  $\beta = dT/dt$ . Substituting into Equation (1) gives the kinetic equation as

$$\frac{d\alpha}{dT} = \frac{A}{\beta} \exp\left(-\frac{E}{RT}\right)(1-\alpha)^n \quad (2)$$

The Coats–Redfern equation is obtained by integrating both sides of Equation (2) and taking logarithmic treatment where the number of reaction stages ( $n$ ) on the right-hand side of Equation is taken as 1, which simplifies to

$$\ln\left[\frac{-\ln(1-\alpha)}{T^2}\right] = \ln\left[\frac{AR}{\beta E}\left(1 - \frac{2RT}{E}\right)\right] - \frac{E}{RT} \quad (3)$$

In particular, it is known from the trial analysis that the first term on the right-hand side of the equation in Equation (3) varies very little in value over the temperature increase interval selected for conventional thermogravimetric experiments, and it can be regarded as a constant. Therefore, Equation (3) can be simplified to a one-dimensional linear equation in the form of

$$Y = b + kX \quad (4)$$

If we make drawings with  $Y = \ln\left[\frac{-\ln(1-\alpha)}{T^2}\right]$  and  $X = \frac{1}{T}$ , a straight line with slope  $k = -\frac{E}{R}$  can be obtained. The reaction activation energy ( $E$ ) can be calculated from the slope ( $k$ ). The calculated activation energy and the fitted intercept can be brought into Equation (3) to calculate the pre-exponential factor ( $A$ ).

### 3.3.2. Analysis of SEM Results

Figure 3 shows the conversion rate curve of carbon black with temperature change when Pt/Pd = 1:1 in the catalyst. From the curve, the decomposition rate between 0 and 10% is almost unchanged with the increase in temperature, the combustion rate is very slow, and the mass consumed at this time is the mass of other impurities such as water in the carbon black. After the decomposition rate rises to 10%, it rises rapidly with the temperature increase. After the decomposition rate reaches 90%, most of the carbon black is already consumed, so the rising trend becomes slower. To make the parameter analysis more reasonable, thermodynamic parameters such as the reaction activation energy ( $E$ ) and pre-exponential factor ( $A$ ) were calculated using data with conversion rates in the range of 10% to 90%.

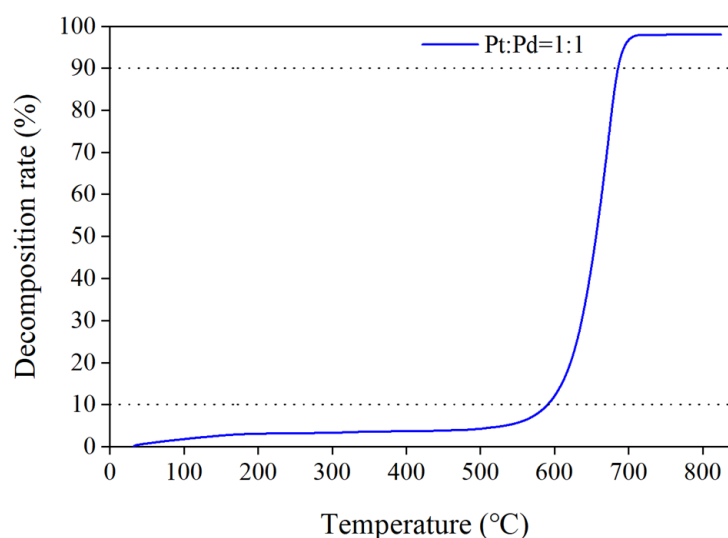


Figure 3. Decomposition rate of carbon black with temperature change.

Figure 4 shows the curves processed and fitted to the experimental data using the Coats–Redfern integration method for the Pt/Pd = 1:1 scheme and the pure carbon smoke, while using the same method to process the data for the other experimental schemes to obtain the kinetic parameters for each experimental scheme, as shown in Table 3, where logarithmic treatment is taken for the pre-exponential factor.

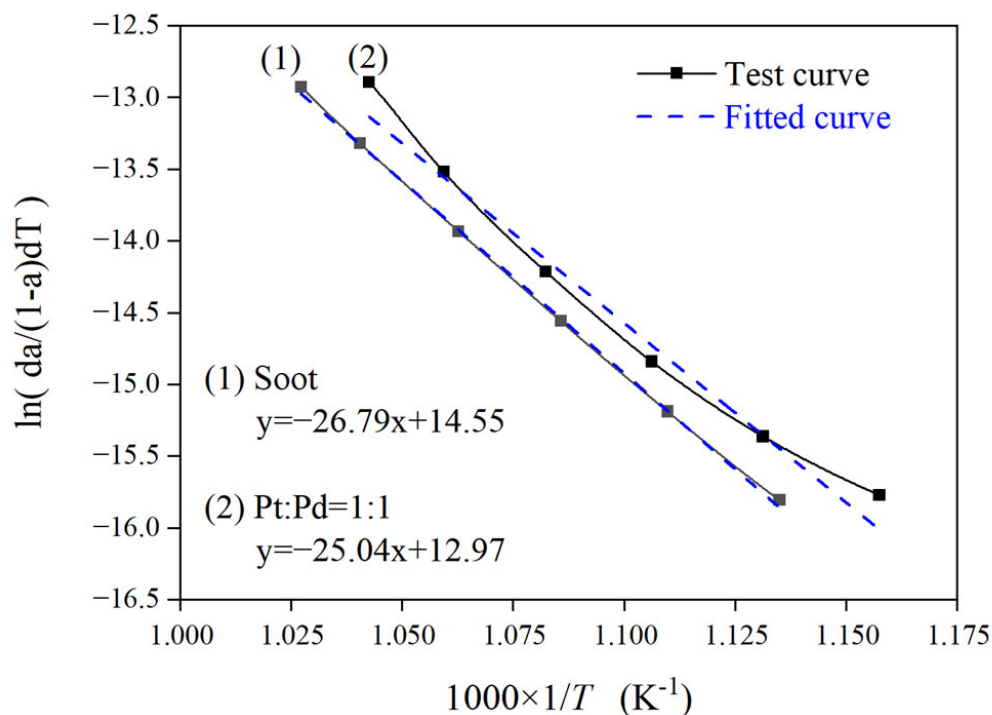


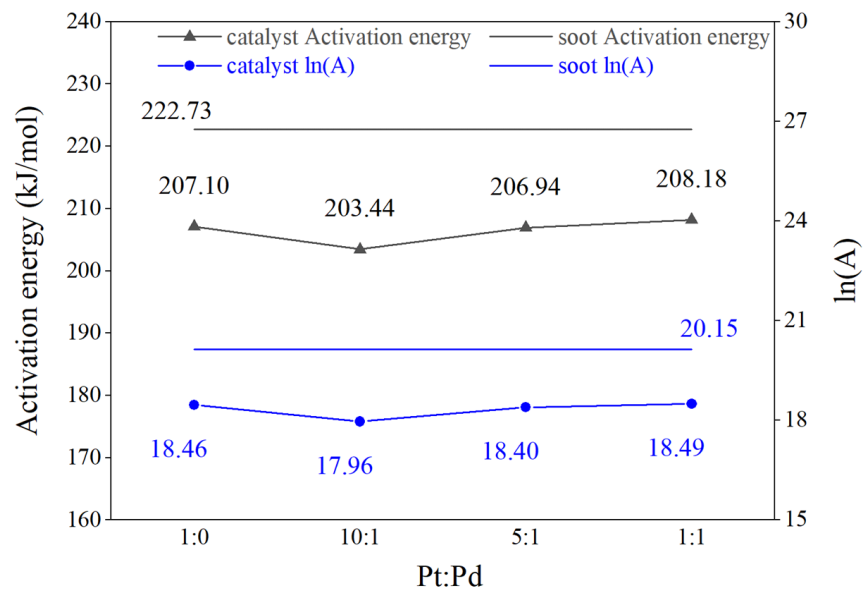
Figure 4. Test curves and corresponding fitted curves.

Table 3. Kinetic parameters of the programs.

Serial Number	Programmatic	Fitted Curve	Activation Energy, E (kJ·mol <sup>-1</sup> )	Pre-Exponential Factor, A (min <sup>-1</sup> )	ln(A)
1	Pt/Pd = 1:0	$y = -24.91x + 12.94$	207.10	$1.04 \times 10^8$	18.46
2	Pt/Pd = 10:1	$y = -24.47x + 12.46$	203.44	$6.31 \times 10^7$	17.96
3	Pt/Pd = 5:1	$y = -24.89x + 12.88$	206.94	$9.77 \times 10^7$	18.40
4	Pt/Pd = 1:1	$y = -25.04x + 12.97$	208.18	$1.08 \times 10^8$	18.49
5	Soot	$y = -26.79x + 14.55$	222.73	$5.58 \times 10^8$	20.14

### 3.3.3. Comparison of Kinetic Parameters and Combustion Temperatures

Figure 5 shows the values of the reaction activation energy and pre-exponential factor for the four Pt/Pd ratio catalyst schemes and the pure carbon fume, where the values of the corresponding parameters for the pure carbon fume are indicated by dashed lines. Reaction activation energy refers to the energy required for the molecules to change from the normal state to the active state in which chemical reactions can easily take place; the lower the activation energy is, the faster the reaction rate is. Therefore, lowering the activation energy will effectively promote the reaction. The pre-exponential factor is the factor representing the total number of effective collisions of activated molecules; the higher the value of the pre-exponential factor, the greater the number of effective collisions of activated molecules, the more easily the reaction is carried out, and the more intense is the degree of the reaction.



**Figure 5.** Kinetic parameters of different Pt/Pd ratio schemes.

The activation energies ( $E$ ) of each scheme are in the range of 203.44–208.18 kJ/mol, and the logarithmic pre-exponential factors ( $\ln(A)$ ) are in the range of 17.96–18.49. Compared with the pure carbon fume, the reaction kinetic parameters of each scheme after doping catalysts are decreased to different extents with the same trend. Among them, the activation energy and logarithmic pre-exponential factor of the Pt/Pd = 10:1 scheme are the lowest at 203.44 kJ/mol and 18.0, respectively, which are 19.29 kJ/mol and 2.19 lower than those of the pure carbon fume.

As can be seen from Figure 4, the addition of a small amount of Pd to the Pt-containing DPF catalyst can rapidly reduce the reaction activation energy of carbon smoke combustion. With the increase in the Pd content, the reaction activation energy of carbon smoke rises and the catalytic effect deteriorates, but the catalytic effect is still obvious compared with that of pure carbon smoke.

Figure 6 shows the starting temperature ( $T_{10}$ ), the final combustion temperature ( $T_{90}$ ), and the peak combustion temperature ( $T_P$ ) of four different Pt/Pd ratios, and  $T_P$  is the temperature of the fastest combustion rate during the combustion of carbon smoke.

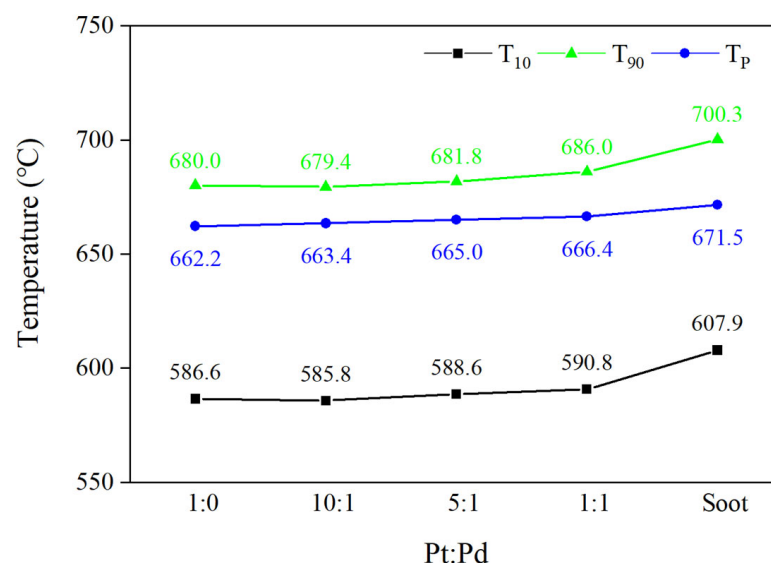


**Figure 6.** Critical temperature points for different Pt/Pd ratio schemes.

The trends of  $T_{10}$  and  $T_{90}$  for the four catalyst schemes are approximately the same as those of the activation energy, with the lowest  $T_{10}$  and  $T_{90}$  for the Pt/Pd = 10:1 scheme at 585.8 °C and 679.4 °C, respectively, and compared with the pure carbon smoke combustion without the catalyst included, both  $T_{10}$  and  $T_{90}$  are drastically reduced by 22.1 °C and 20.9 °C, respectively. The use of Pt- and Pd-doped catalysts can effectively reduce the ignition temperature of carbon smoke and promote the passive regeneration of DPF. The  $T_P$  of the four scenarios does not differ much from that of the pure carbon smoke case, with only a slight decrease, among which the lowest  $T_P$  scenario is Pt/Pd = 1:0 with a temperature of 662.2 °C, which is 9.3 °C lower than that of the pure carbon smoke case.

#### 4. Conclusions

This paper focuses on analyzing the characterization of different Pt-Pd catalysts and their catalytic performance on soot. Several conclusions are as follows:

1. Pt-Pd has a good synergistic effect, and the doping of Pt-based catalysts with Pd can improve the dispersion of the catalysts, significantly increase the specific surface area, and reduce the activation energy and reaction temperature of the soot reaction, but excessive doping of Pd will lead to the enhancement of the agglomeration effect of the catalysts, a reduction in the specific surface area, and an increase in the activation energy and reaction temperature of the soot reaction;
2. When the ratio of Pt/Pd was 10:1, the specific surface area and the pore volume of the catalyst were the largest, and the activation energy of combustion and the pre-exponential factor of carbon soot particles were the smallest, which were 203.44 kJ/mol and  $6.31 \times 10^7$ , respectively, and were 19.29 kJ/mol and  $4.95 \times 10^8$  lower than those of pure carbon soot. At the same time, the starting temperature of the soot,  $T_{10}$ , and the final temperature of the carbon soot,  $T_{90}$ , were the lowest, which were 585.8 °C and 679.4 °C, respectively: 22.1 °C and 20.9 °C lower than those of pure carbon smoke;
3. The activation energies of the four different Pt-Pd catalysts range from 203 kJ/mol to 209 kJ/mol, with the pre-exponential factor between  $6.31 \times 10^7$  and  $1.08 \times 10^8$ , and the temperature range of 580 °C to 690 °C is the main temperature range for the catalytic combustion of carbon smoke.

From the comprehensive results of the full analysis, the ratio scheme of Pt/Pd = 10:1 has the lowest activation energy,  $T_{10}$ , and  $T_{90}$  for the soot combustion reaction, the highest exothermic rate, and the most active reaction, which is the best scheme for the passive regeneration catalyst of DPFs. Further studies on different doping modes of other elements, including non-noble metals, will be conducted in the future.

**Author Contributions:** Conceptualization, D.L., Y.Z. and K.X.; methodology, K.X.; software, K.X. and G.S.; validation, K.X.; formal analysis, K.X.; investigation, Y.Z. and G.S.; writing—original draft preparation, K.X. and K.Z.; writing—review and editing, K.Z.; supervision, D.L.; project administration, Y.Z. All authors have read and agreed to the published version of the manuscript.

**Funding:** This research was funded by the National Key R&D Program of China, grant number 2022YFE0100100; the National Natural Science Foundation of China, grant number 52206167.

**Data Availability Statement:** The raw data supporting the conclusions of this article will be made available by the authors on request.

**Conflicts of Interest:** The authors declare no conflicts of interest.

#### References

1. Ministry of Ecology and Environment of the People's Republic of China. 2022 Annual Report on Environmental Management of Mobile Sources in China. Available online: [https://www.mee.gov.cn/hjzl/sthjzk/ydyhjgl/202212/t20221207\\_1007111.shtml](https://www.mee.gov.cn/hjzl/sthjzk/ydyhjgl/202212/t20221207_1007111.shtml) (accessed on 7 December 2022).
2. Khobragade, R.; Singh, S.K.; Shukla, P.C.; Gupta, T.; Al-Fatesh, A.S.; Agarwal, A.K.; Labhasetwar, N.K. Chemical composition of diesel particulate matter and its control. *Catal. Rev.* **2019**, *61*, 447–515. [CrossRef]

3. Niessner, R. The many faces of soot: Characterization of soot nanoparticles produced by engines. *Angew. Chem. Int. Ed.* **2014**, *53*, 12366–12379. [[CrossRef](#)] [[PubMed](#)]
4. Bond, T.C.; Doherty, S.J.; Fahey, D.W.; Forster, P.M.; Bernsten, T.; DeAngelo, B.J.; Flanner, M.G.; Ghan, S.; Kärcher, B.; Koch, D.; et al. Bounding the role of black carbon in the climate system: A scientific assessment. *J. Geophys. Res. Atmos.* **2013**, *118*, 5380–5552. [[CrossRef](#)]
5. Zhong, H.; Tan, J.W.; Wang, Y.L.; Tian, J.L.; Hu, N.T.; Cheng, J.; Zhang, X.M. Effects of a diesel particulate filter on emission characteristics of a China II non-road diesel engine. *Energy Fuel* **2017**, *31*, 9833–9839. [[CrossRef](#)]
6. Wang, Z.B.; Liu, P.; Li, H.M.; Li, R.; Pan, X.B.; Zhao, Y. The development of diesel particulate filter technology. *IOP Conf. Ser. Earth Environ. Sci.* **2021**, *632*, 032012. [[CrossRef](#)]
7. Feng, N.J.; Meng, J.; Wu, Y.; Chen, C.; Wang, L.; Gao, L.; Wan, H.; Guan, G.F. KNO<sub>3</sub> supported on three-dimensionally ordered macroporous La<sub>0.8</sub>Ce<sub>0.2</sub>Mn<sub>1-x</sub>Fe<sub>x</sub>O<sub>3</sub> for soot removal. *Catal. Sci. Technol.* **2016**, *6*, 2930–2941. [[CrossRef](#)]
8. Li, Q.; Meng, M.; Xian, H.; Tsubaki, N.; Li, X.G.; Xie, Y.N.; Hu, T.D.; Zhang, J. Hydrotalcite-Derived Mn<sub>x</sub>Mg<sub>3-x</sub>AlO Catalysts Used for Soot Combustion, NO<sub>x</sub> Storage and Simultaneous Soot-NO<sub>x</sub> Removal. *Environ. Sci. Technol.* **2010**, *44*, 4747–4752. [[CrossRef](#)]
9. Lee, J.H.; Lee, S.H.; Choung, J.W.; Kim, C.H.; Lee, K.Y. Ag-incorporated macroporous CeO<sub>2</sub> catalysts for soot oxidation: Effects of Ag amount on the generation of active oxygen species. *Appl. Catal. B Environ.* **2019**, *246*, 356–366. [[CrossRef](#)]
10. Lin, X.T.; Li, S.J.; He, H.; Wu, Z.; Wu, J.L.; Chen, L.M.; Ye, D.Q.; Fu, M.L. Evolution of oxygen vacancies in MnO<sub>x</sub>-CeO<sub>2</sub> mixed oxides for soot oxidation. *Appl. Catal. B Environ.* **2018**, *223*, 91–102. [[CrossRef](#)]
11. Qi, B.Y.; Li, Z.G.; Lou, D.M.; Zhang, Y.H. Experimental investigation on the effects of DPF Cs-V-based non-precious metal catalysts and their coating forms on non-road diesel engine emission characteristics. *Environ. Sci. Pollut. Res.* **2023**, *30*, 9401–9415. [[CrossRef](#)] [[PubMed](#)]
12. Wagloehner, S.; Baer, J.N.; Kureti, S. Structure–activity relation of iron oxide catalysts in soot oxidation. *Appl. Catal. B Environ.* **2014**, *147*, 1000–1008. [[CrossRef](#)]
13. Ji, F.; Men, Y.; Wang, J.G.; Sun, Y.L.; Wang, Z.D.; Zhao, B.; Tao, X.T.; Xu, G.J. Promoting diesel soot combustion efficiency by tailoring the shapes and crystal facets of nanoscale Mn<sub>3</sub>O<sub>4</sub>. *Appl. Catal. B Environ.* **2019**, *242*, 227–237. [[CrossRef](#)]
14. Oi-Uchisawa, J.; Wang, S.D.; Nanba, T.; Ohi, A.; Obuchi, A. Improvement of Pt catalyst for soot oxidation using mixed oxide as a support. *Appl. Catal. B Environ.* **2003**, *44*, 207–215. [[CrossRef](#)]
15. Wang, K.X. Low-Temperature Activity and Sulfur Resistance of Non-Precious Metal CDPF Catalysts for the Catalytic Oxidation of Carbonaceous Smoke. Master’s Thesis, Shanghai Jiao Tong University, Shanghai, China, 2019.
16. Oi-Uchisawa, J.; Obuchi, A.; Wang, S.; Nanba, T.; Ohi, A. Catalytic performance of Pt/MO<sub>x</sub> loaded over SiC-DPF for soot oxidation. *Appl. Catal. B Environ.* **2003**, *43*, 117–129. [[CrossRef](#)]
17. Zhang, Y.H.; Lou, D.M.; Tan, P.Q.; Hu, Z.Y.; Fang, L. Effect of catalyzed diesel particulate filter and its catalyst loading on emission characteristics of a non-road diesel engine. *J. Environ. Sci.* **2023**, *126*, 794–805. [[CrossRef](#)] [[PubMed](#)]
18. Lim, C.B.; Kusaba, H.; Einaga, H.; Teraoka, Y. Catalytic performance of supported precious metal catalysts for the combustion of diesel particulate matter. *Catal. Today* **2011**, *175*, 106–111. [[CrossRef](#)]
19. Kaneeda, M.; Iizuka, H.; Hiratsuka, T.; Shinotsuka, N.; Arai, M. Improvement of thermal stability of NO oxidation Pt/Al<sub>2</sub>O<sub>3</sub> catalyst by addition of Pd. *Appl. Catal. B Environ.* **2009**, *90*, 564–569. [[CrossRef](#)]
20. Yashnik, S.A.; Ismagilov, Z.R. Pt–Pd/MnO<sub>x</sub>–Al<sub>2</sub>O<sub>3</sub> oxidation catalysts: Prospects of application for control of the soot emission with diesel exhaust gases. *Kinet. Catal.* **2019**, *60*, 453–464. [[CrossRef](#)]
21. Meng, Z.W.; Yang, D.; Yan, Y. Comparison of methods for analyzing the kinetic response of diesel particles to oxidation. *J. Xihua Univ. (Nat. Sci. Ed.)* **2013**, *32*, 51–55.

**Disclaimer/Publisher’s Note:** The statements, opinions and data contained in all publications are solely those of the individual author(s) and contributor(s) and not of MDPI and/or the editor(s). MDPI and/or the editor(s) disclaim responsibility for any injury to people or property resulting from any ideas, methods, instructions or products referred to in the content.